RT E JOURNAL

Enhancing productivity in Laser Powder Bed Fusion (PBF-LB/M) via layerwise Laser Remelting – proof of concept

Alexander Schmidt [a], Lennart Schmidtsdorff [a], Sebastian Härtel [a]

[a] Chair of Hybrid Manufacturing Brandenburg University of Technology, 03046 Cottbus, Germany

Abstract A limiting factor for a widespread application of laser powder bed fusion (PBF-LB/M) is the necessary compromise between quality and productivity resulting in high manufacturing costs. The productivity can be enhanced by increasing the layer height. However, this adjustment may result in either insufficient bonding due to inadequate laser energy input for complete melting or in an increased surface roughness and porosity through excessive energy density. The increased energy input required for complete melting of a high layer height induces the Marangoni effect which promotes an increase in surface roughness of the interlayer. Interlayer roughness peaks act as undercuts regarding the recoating process and result in local low density of the powder bed and thus porosity. Therefore, the requirements for a laser exposure are an adequate melt pool depth and a sufficient interlayer surface quality. For high layer heights and thus high productivity it is not possible to meet both requirements with a state of the art exposure strategy.

This work studied the feasibility of using layerwise laser remelting to smooth out roughness peaks after the first laser exposure with high energy density when using high layer height. A positive impact of the laser remelting on penetration depth and porosity was observed. Copper samples printed using the remelting strategy and a layer height of 60 µm achieved comparable values of porosity as samples with a layer height of 30 µm and a state of the art melting strategy. This approach resulted in time savings of 28 % while maintaining high part quality.

State of the art regarding increasing the PBF-LB efficiency

Numerous technological advantages of additive manufacturing (AM), such as near-net-shape production of complex geometries, the use of multi-materials, the incorporation of honeycomb structures, and a high degree of customization, result in the rapid development and introduction of the corresponding systems into today's industry. While the availability and range of specially developed systems is already very comprehensive, the fields of application are still very limited. Thus, AM technology is underrepresented compared to conventional manufacturing processes, particularly in the field of mass production. Specifically, the application areas of Laser Powder Bed Fusion (PBF-LB) are limited to the production of high-quality and high-priced components such as for aerospace, medical, tooling or energy applications. Here PBF-LB is used to produce highly complex metal parts that cannot be realized through casting or machining, with mechanical properties comparable to parts produced from bulk material [1]. Due to high thermal and electric conductivity of copper, possible application areas of copper AM-parts are thermal dissipation solutions and electronic components in automotive, aerospace, and energy sectors [2-4]. However, it's industry-wide application is hindered by the low build rate and thus high production cost.

The process time consists primarily of the coating time and the laser exposure time which depends on the laser scanning speed, hatch distance and mainly the layer thickness. Thus, a common approach to increase the deposition rate is the use of multiple lasers, which significantly reduces the build time [5-7]. Here, each laser is assigned to a specific region of the same build plate, enabling parallel processing of one part in different regions or several AM-parts simultaneously. By the distribution of the exposure workload among multiple lasers, this approach significantly reduces the exposure time while the coating time remains the same. As the coating time remains unchanged, the use of two lasers does not necessarily result in a 50 % reduction in the total build time. In their work, Wong et al. report a 63 % reduction in the build time of PBF-LB processes when using four lasers and a layer height of 30 µm, with little to no compromise in the mechanical properties of the specimens [5]. This approach is already used in industry and therefore represents the state of the art. Its disadvantages include higher investment costs and increased thermal input per unit time, which may be critical.

The application of multiple lasers for the exposure process may be combined with the parallelization of the coating and exposure processes. Here, the coating process and the exposure process take place simultaneously. Both the application of multiple lasers and the process parallelization reduce the total process time. This approach represents the state of the art and is offered by system providers such as Renishaw. According to Renishaw, this approach may increase the build rate by up to 50%, depending on the component geometry [8].

Common PBF-LB devices use a mono-directional coating process. Since the productivity depends, among other factors, on the coating time, a bi-directional coating process may reduce the total process time and thus increase the process efficiency. *Figure 1* shows the principles of PBF-LB processes with a) a mono-directional and b) bi-directional coating processes. Mono-directional coating processes use a powder storage and a powder overflow container, *Fig. 1 a)*. Here the coating blade first moves from the storage container across the build plate toward the overflow container, thus coating the powder bed with the desired layer height. To ensure that the coating blade carries enough powder for the entire build plate, the theoretically required powder quantity is multiplied by a safety factor. The excess powder ends up in the overflow container and the coating blade then moves back

to the storage container. After the coating process described, the laser exposure takes place. For the case of bi-directional coating, two storage containers are used instead of one storage and one overflow container, *Fig. 1 b)*. Both containers serve as storage and overflow container at the same time and are height-adjustable accordingly. This arrangement of powder containers enables the bi-directional coating and thus saves the travel time from the overflow to the storage container. The disadvantage of bi-directional coating is a higher construction effort and thus higher system price.

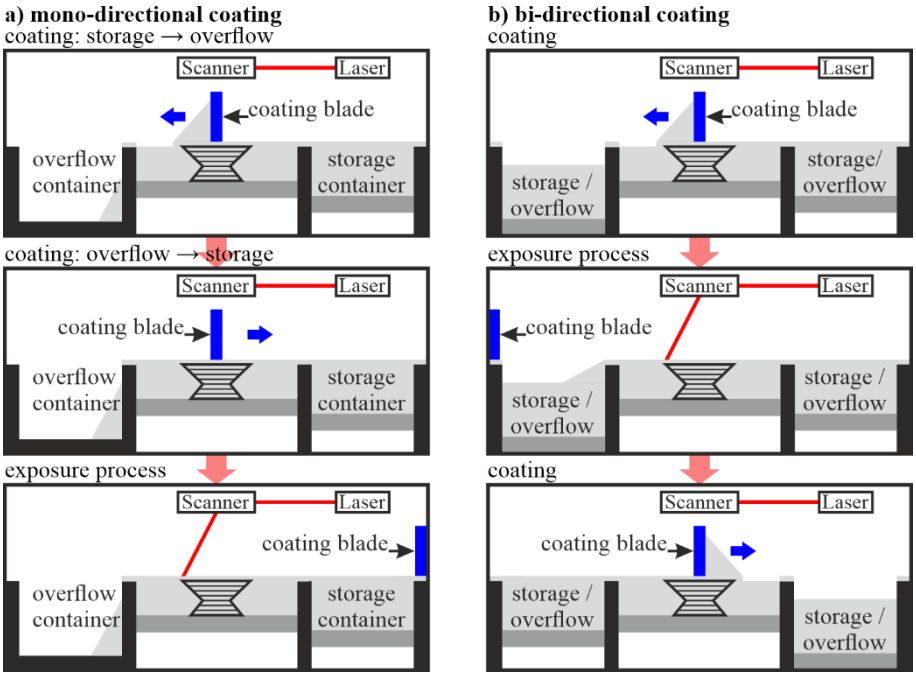

Figure 1: Principle of PBF-LB processes with a) mono-directional and b) bi-directional coating

Due to the flow characteristics of the powder, the coating velocity is limited. The flow characteristics of powders depend on the particle size distribution, particle shape, chemical composition, humidity, and temperature. Exceeding the maximal permissible coating speed results in a lower powder bed quality. Therefore, one approach to increase the process efficiency is to improve the flowability of the powder used and thus accelerate the coating process. Specifically, the coating blade and thus the powder bed are subjected to ultrasonic vibrations [9].

In their publication Herzog et al. suggest a combined approach of PBF-LB and subsequent Hot Isostatic Pressing (HIP) process as a method to improve the overall productivity [10]. HIP is a manufacturing process in which metallic materials are subjected to compressive stresses at high gas pressures and high temperatures to increase the density, eliminate defects such as porosity and achieve homogeneous properties. This process is applied to conventionally manufactured but also AM-parts, especially in aerospace applications. According to this approach, the PBF-LB process parameters for Ti-6Al-4V were optimized to increase the scanning speed, which ensures a density above 95 % in the as-build state. By the subsequent HIP process the density was improved to a value of 99.8 %. In detail the PBF-LB scanning speed was increased by 67 % which resulted in an overall time saving of 26 % in consideration of the HIP treatment time. Here, the disadvantage are the higher investment costs for an additional post treatment device in the production chain such as a HIP device and a volume shrinkage of the AM-part while HIP.

The combination of conventional processes such as casting and machining with a PBF-LB process offers a possibility for increasing the overall productivity. Within such hybrid production chains, a conventional semi-finished product with simple geometry is first manufactured and subsequent further complex geometry is then added with a PBF-LB process to finish the product. The challenges here are (a) the mounting of the semi-finished products on the build plate within the PBF-LB device and (b) the alignment of the semi-finished product with the added AM-part to ensure the laser scans the correct cross section. For these purposes a build plate enabling the mounting and an optical calibration system were developed in the industry [11, 12]. This approach offers the potential to increase the overall productivity for the case of AM-parts which might be divided in semi-finished products with simple geometries and complex shaped parts. Furthermore, some investments for such systems are necessary.

Another possibility to improve the economic efficiency by a hybrid manufacturing process chain is the combination of a Transient Liquid Phase (TLP) bonding with a HIP-process according to [13]. By bonding one PBF-LB part of a complex geometry with another conventionally manufactured part while performing a HIP-process the overall economic efficiency of the process chain is increased. According to the state of the art, a metallurgical bond is not possible during a HIP-process. Due to the applied high pressure during a HIP-process the respective gas penetrates the interface between the parts. Here the gas prevents the interactions between the metallic parts and thus the formation of a metallurgical bond. TLP-bonding is a joining process characterized by high bond quality, with properties comparable to those of the base material. The process starts with the melting of the filler metal and is followed by the dissolution of the base material by the liquid filer metal. Once the diffusion of the filler metal elements into the base material is pronounced, an isothermal solidification of the filler metal occurs. Due to isothermal solidification, the remelting temperature of the joint is higher than the processing temperature. As a result, this process is suitable for high-stress and high-temperature applications, such as those in the aerospace and energy sectors [14-16]. Therefore, the authors suggest to apply a TLP-process in a HIP-device with a low pressure to seal the interface between two metallic geometries by the solidification of the filler metal in the first step and thus to prevent the gas penetration into the interface during the subsequent HIP-process, *Fig. 2*.

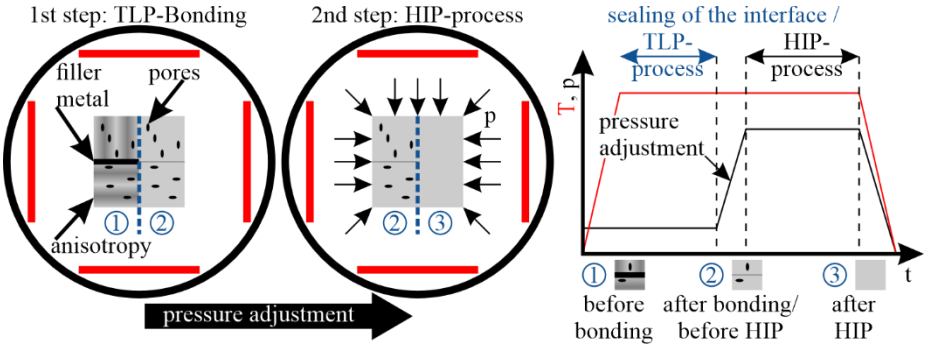

Figure 2: Principle of a hybrid TLP-HIP-process, according to [13]

Regarding the TLP-joint the subsequent HIP-process acts as a heat treatment and particularly the high pressure results in an improvement of the thermo-mechanical bond properties and thus superior joint quality compared to conventional bonding processes such as brazing or welding [17, 18]. Two application cases are suggested. The first one is the bonding of two or more PBF-LB part for the reason of manufacturing big PBF-LB parts

and thus to overcome the technical limitation of the PBF-LB technology regarding the part size. The second application case involves bonding a PBF-LB part with a complex geometry to a conventionally manufactured component with a simple shaped geometry in order to increase the overall economic efficiency. The disadvantage is the requirement for additional systems to perform the HIP-process within the production chain. Therefore, in terms of economic efficiency, the applications of the described TLP-HIP approach are limited to PBF-LB parts which require a HIP-process from the start.

The approaches described above aim to increase the economic efficiency and are technically feasible. The disadvantages are the respective limited areas of application or the necessity for additional investments. For the case of existing facilities one of the most effective and most straightforward strategies to improve the efficiency of powder bed fusion processes is by process parameters optimization, primarily by increasing the layer height. Therefore, efforts were made in academia and industry in the last years for different materials to determine process parameter sets meeting an acceptable compromise between quality and efficiency [19-24].

1 Proposed LR-approach for increasing the efficiency

Conventional PBF-LB processes for aluminum and nickel alloys or steels may utilize layer thicknesses above 50 µm. For the case of pure copper the layer thickness is typically 20-30 µm due to the low absorption rate of the material. When using a wavelength of 1094 nm, corresponding to infrared laser, the layer thickness is approximately 20 µm [2-4]. In the case of a green laser, which exhibits a higher absorption rate, the literature reports layer thicknesses of 30 µm [25, 26].

According to the literature, typical pouring densities of the powder bed in PBF-LB processes range from 50-60% [27-29]. The low pouring density results in an increase of the real powder bed layer height, even though the nominal layer thickness remains constant throughout the height of the AM-part. In detail, assuming a conservative pouring density of 50%, and a fully dense (100%) AM-part, the real powder bed layer height converges to approximately twice the nominal layer height within ten layers, as shown exemplarily for the first three layers in *Figure 3*.

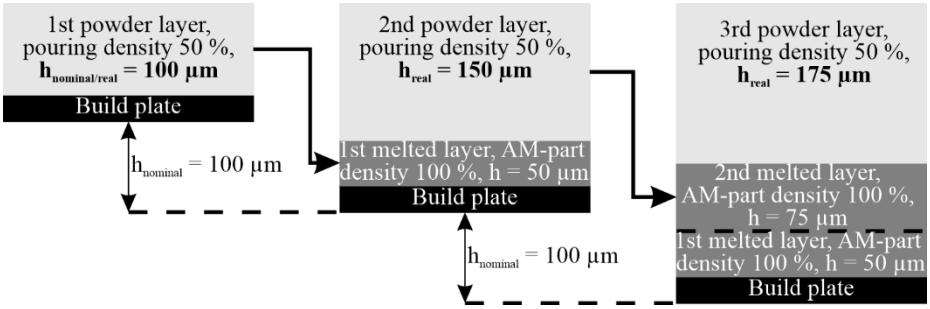

Figure 3: Increase of the real layer height due to pouring density

Here, a pouring density of 50 % and a nominal layer height of $h_{nominal}$ = 100 µm were considered. Already within the third layer, the real layer height is h_{real} = 175 µm. Therefore, the melt pool depth is typically at least two to three times higher than the nominal layer height, ensuring every layer undergoes at least one and preferably several full melting cycle. For the case of a keyhole mode material evaporation and thus material loss results in further increase of the real layer height. For a stable conduction mode PBF-LB process, material evaporation and spattering effects can be considered negligible.

The combination of low layer height and state of the art scanning parameters guarantees sufficient bonding between the layers, low porosity, and a smooth surface roughness at the cost of efficiency as shown in *Figure 4*. For simplicity, the representation of the height loss due to pouring density was omitted here. During the first exposure of the respective layer pores may arise. Due to the low layer height, each layer undergoes several full melting cycles, which results in the elimination of residual pores of a specific layer during the exposure of the next layer.

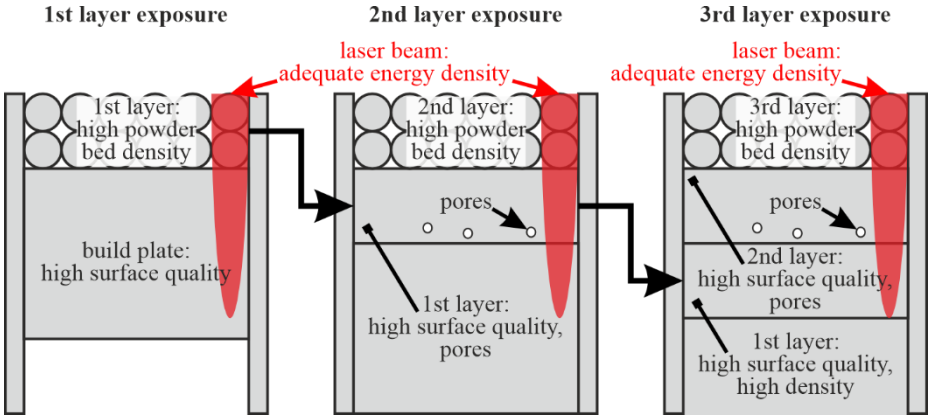

Figure 4: PBF-LB process according to the state of the art:
low layer height and state of the art exposure strategy
→ low efficiency, high quality of the AM-part

Figure 5 shows a PBF-LB process with a triple layer thickness and a state of the art exposure strategy. On the one hand the increase of layer height results in an efficiency increase. On the other hand, an increase in layer height without adapting scanning parameters such as laser power, hatch distance or scanning speed result in a significant rise in lack-of-fusion defects and pores, negatively impacting the final part's thermo-mechanical performance. The reasons are a low melt pool depth and a short liquid lifetime resulting from an insufficient energy input, particularly in the bottom of the respective layer. Here each layer is melted only once and thus the liquid life time is shortened. For the case of low melt pool depth interlayer bonding defects arise.

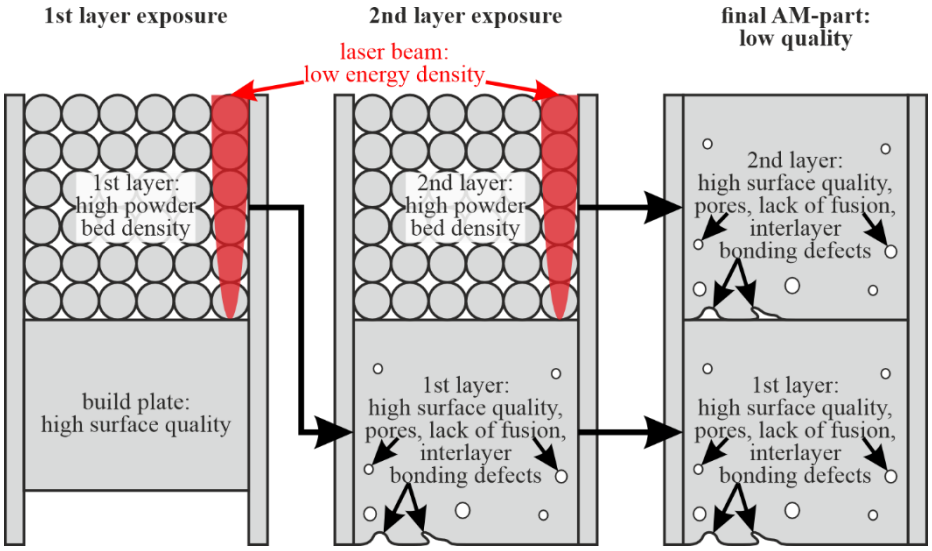

Figure 5: PBF-LB process with triple layer height and state of the art exposure strategy:
→ high efficiency, low quality of the AM-part due to low energy density

Figure 6 shows a PBF-LB process with a triple layer thickness and a high laser energy density. An increase in laser energy input is necessary to achieve a regarding higher layer thickness sufficient melt pool depth and thus liquid life time during the process. The high melt pool depth ensures sufficient bonding of the first layer to the build plate or between the subsequent layers. The adequate liquid life time prevents the formation of lack of fusion defects. However, the increased heat input in turn promotes the occurrence of an excessive Marangoni flow, a convection within the molten material which results in elevated surface roughness and porosity and may destabilize the melt pool itself [30-32]. The increased surface roughness degrades the powder bed quality of the following layer. In detail the roughness peaks act as undercuts regarding the recoating process and result in local low density of the powder bed which promotes pore formation during the exposure process and interlayer bonding defects. Therefore, efforts to increase throughput by increasing the layer height when using the state of the art exposure strategy with low or high laser energy density result in decreased part quality, such as increased porosity and surface roughness.

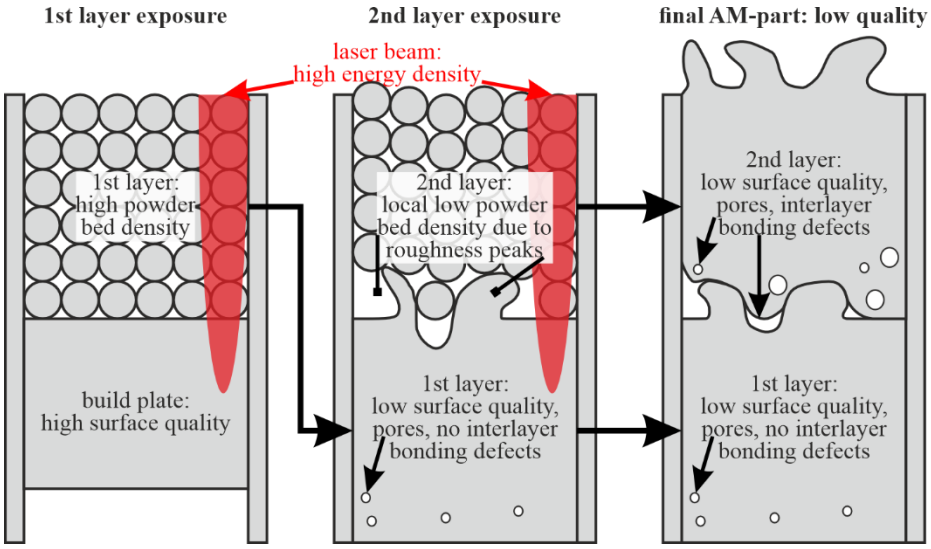

Figure 6: PBF-LB process with triple layer height and high laser energy density:
→ high efficiency, low quality of the AM-part due to low powder bed quality

Thus, when employing state of the art exposure strategies, the achievable layer height and thus the process efficiency is limited. On the one hand, the limited melt pool depth constrains the maximum achievable layer thickness. Conversely, increasing the melt pool thickness as required results in elevated surface roughness, which in turn compromises powder bed quality. To resolve the inherent conflicts in the exposure process associated with elevated layer thicknesses, the following approach is proposed.

Figure 7 shows a PBF-LB process with triple layer height and a layerwise laser remelting (LR) exposure strategy. The layerwise LR-application aims to reduce the occurring roughness induced by high energy input by smoothing out roughness peaks. Here, the first laser exposure with a high laser energy density ensures a sufficient depth of the melt pool and thus prevents interlayer bonding defects. The LR-application serves to provide a sufficient surface quality for the next coating process and thus enables a high powder bed density. The approach is similar to that of laser polishing, where the top surface of a metallic object is remelted using a laser beam to improve the surface quality [33-36]. Furthermore, the LR-application prolongs the liquid life time and ensures every layer undergoes at least two full melting cycles. Thus, the described LR-approach allows the application of higher layer thicknesses while maintaining high powder bed quality and

sufficient melt pool depth, and consequently high AM-part quality. Since the LR strategy is a software-based solution, it may be implemented in all beam-based powder bed systems such as laser or electron beam powder bed.

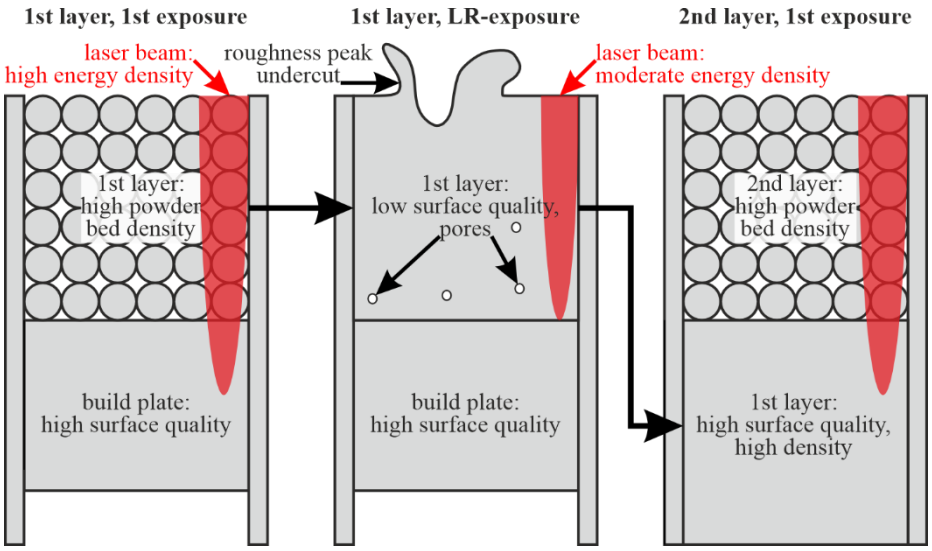

Figure 7: PBF-LB process with triple layer height and LR-application:
→ high efficiency and high quality of the AM-part

Table 1 provides a qualitative comparison between state of the art (SoA) PBF-LB deposition rates and those of the proposed approach on the basis of number of required coating and exposure processes. Here, an increase of the layer height from h_{SoA} = 30 µm to h_{LR} = 90 µm is considered. An AM-part with a height of 180 µm is taken as a representative example. In this example the coating time is reduced by 67 %. The number of required exposure processes is reduced by 34 %. It should be noted that the exposure times of the SoA exposure and the LR-application may differ. Therefore, a quantitative indication of the time savings of the exposure process is not possible in general but only for specific parameter sets.

Table 1: Qualitative comparison of the deposition rates between SoA and the LR-approach

	State of the art (SoA)	LR-approach
AM-part height [µm]	180	180
Layer height [µm]	30	90
Number of required layers [-]	6	2
Number of required coating processes [-]	6 (= 100 %)	2 (= 33 % relative to SoA)
Number of required exposure processes [-]	6 (= 100 %)	4 (= 66 % relative to SoA)

LR-application in PBF-LB takes place by scanning and thus remelting an already solidified layer or part of a layer after the first laser exposure. The goal of LR is to homogenize the material, refine the grain structure, create a material gradient between two materials, and reduce porosity or surface roughness of the interlayer or top layer of AM-parts at a cost of longer production times [37-40]. Yasa et al. report on the layerwise LR-application during a PBF-LB process with AISI 316L material, achieving 100 % density of the AM-part and to improve the surface roughness by approximately 90 % [37]. In their work Chen et al.

describe the influence of LR-application on the grain size of AM-parts manufactured of pure Tantalum for medical applications. In detail the average grain size was reduced by 15.7 % - 18.8 % [38]. Further studies demonstrate that LR-application results in an increased in-situ mixing degree in the melt pool. Two application cases are described. First one is the homogenization of NiTi-parts for the medical sector fabricated from elemental nickel and titanium powders. Here the LR-application results in more homogeneous microstructure regarding the element distribution [39]. The second one is the manufacturing of functionally graded AM-parts by applying LR in the interface between two different materials [40].

The possibility to smooth the surface roughness by in-situ LR-application during a PBF-LB process is decisive for this approach and is proven according to the state of the art. Thus, the basic condition for the application of this approach is regarding the respective layer height sufficient melt pool depth during the first laser exposure and during the LR-application. For the case of a keyhole mode PBF-LB process the melt pool depth is proven to be in dependence of the process parameter typically up to two to three times bigger than the actual layer height. But for the case of a conduction mode PBF-LB process, the melt pool depth is limited by the low thermal conductivity of the powder bed. On the other hand, due to the lower density of a powder bed compared to the density of bulk material, the melting of loose powder requires less energy than the melting of bulk material. Therefore, there is a chance to increase the overall melt pool depth by increasing the layer height. Moreover, after the first exposure and thus during the LR-exposure the thermal conductivity of the respective layer is expected to be higher. Another relevant difference between the first exposure and the LR-application are the temperatures and the temperature gradients. In detail, regarding the LR application, the first exposure process acts as a preheating step for the respective layer and may therefore result in higher initial temperatures and lower temperature gradients during the LR application. Therefore, the melt pool depth is expected to be higher after the LR-application compared to the case of the first exposure.

The aim of this study is to evaluate the melt pool depth during first exposure of the powder bed and during LR-exposure of AM-layers in dependence of the process parameters, including different layer heights and energy densities and thereby to assess the applicability of the described LR-approach for the case of a conduction mode PBF-LB process.

2 Experimental setup

2.1 Material and AM-device

The material used in this study was pure (99,9 %) copper powder. According to the data sheet the powder as supplied exhibited a particle size distribution ranging from 10-63 µm, *Fig. 8 a)*. The powder primarily consisted of spherical particles, but aspherical powder agglomerates with the size up to >100 µm were observed during analysis of the powder before the AM-process, *Fig. 8 b)*. Such powder with aspherical agglomerates has reduced flow characteristics which results in a low powder bed density and thus formation of big pores.

The AM-system used for the PBF-LB process consisted of an AconityMINI (Aconity3D GmbH, Germany) equipped with a TruDisk 1020 laser (TRUMPF SE + Co. KG, Germany), which operates at a wavelength of 532 nm corresponding to a green laser. The laser delivers a maximum power output of 1000 W and has a spot size in the range of 200 µm.

Pure Argon with an oxygen content below 200 ppm O_2 was used as shielding gas during the process. A pure copper substrate served as build plate.

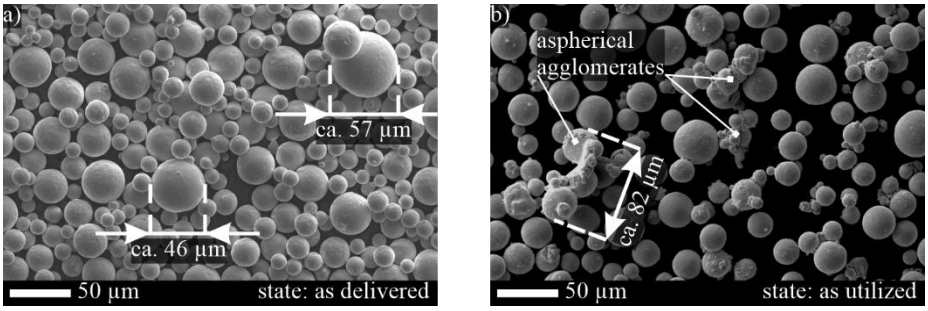

Figure 8: SEM-images of Cu-powder: a) as delivered without agglomerates and b) as utilized in the AM-process with aspherical agglomerates

2.2 PBF-LB process parameter and LR-implementation

The powder was applied using a carbon fibre recoater blade. A constant hatching distance of 100 µm was used during the study and a simple hatching strategy with 3 perimeters, rotating by 67° every layer, was utilized. The LR-strategy was implemented by overlaying two distinct geometries within the machine software application. The LR-hatching pattern was rotated by 90° relative to the initial exposure pattern.

The samples geometry consisted of a cuboid with a base of A = 10 x 10 mm and a height of h = 3 mm. All samples were metallographically prepared and each sample was additionally etched using KLEMM-III etchant to highlight the grain boundaries and allow for measurement of the respective melt pool depth. The melt pool depth was calculated as the average of 10 evenly distributed measuring points along the sample cross section. A digital microscope (VH-X-7000, Keyence, Japan) was utilized to obtain cross-sectional images of the samples and evaluate the porosity values.

All of the process parameters employed are presented in *Table 2*. The first three samples aimed on the characterization of the reference parameter set. The reference parameter set was chosen on the basis of a previous study to improve the process stability and the part properties for AM of copper with the AM-device employed in this study. Furthermore, samples manufactured with the V1 parameter set served to evaluate the impact of the current powder condition on the AM-part quality. For this purpose, four samples with V1 parameter set were manufactured. V1, with a layer height of 30 µm, represented the first AM-process condition in the initial layers for which the real layer height corresponds to the nominal layer height. To take the increase of the real layer height due to pouring density in account and to evaluate the influence of the layer height on the melt pool depth nominal layer heights of 60 µm (V2) and 90 µm (V3) were utilized, *Table 2*. The parameter sets V4-V7 were employed to investigate the influence of the track energy on the melt pool depth without a LR-application with a constant layer height of h_L = 30 µm, *Table 2*. To evaluate the influence of the layer height on the melt pool depth at the respective energy levels in the third and fourth sample sets the layer height was varied at two further levels at discrete energy levels of $E_{s,1}$ = 1.0 J/mm and $E_{s,2}$ = 1.25 J/mm, *Table 2*. The track energy (E_T) is defined as the quotient of laser power (P) and the scan speed (v). To investigate the influence of a layerwise LR-application on the melt pool depth and to compare the quality of the LR-samples with the state of the art regarding porosity, further samples were manufactured using the LR-exposure strategy, *Table 2*. For the comparison of LR-samples with the state of the art, the V1 parameter set represented the state of the art.

Table 2: Process parameter

Process	Layer height [µm]	Exposure	Power [W]	Speed [mm/s]	Track energy [J/mm]	Objective
V1	30	1st	800	1,000	0.8	Characterization of the reference parameter set with respect to melt pool depth at different AM-part heights, influence of layer height on the melt pool depth
		LR	Not applied			
V2	60	1st	800	1,000	0.8	
		LR	Not applied			
V3	90	1st	800	1,000	0.8	
		LR	Not applied			
V4	30	1st	1,000	1,000	1.0	Influence of energy level on the melt pool depth and evaluation of possible process window regarding the track energy
		LR	Not applied			
V5	30	1st	1,000	800	1.25	
		LR	Not applied			
V6	30	1st	800	640	1.25	
		LR	No applied			
V7	30	1st	1,000	715	1.4	
		LR	Not applied			
V8	60	1st	1,000	1,000	1.0	Influence of layer height on the melt pool depth at track energy value of Es = 1.0 J/mm
		LR	Not applied			
V9	90	1st	1,000	1,000	1.0	
		LR	Not applied			
V10	60	1st	800	640	1.25	Influence of layer height on the melt pool depth at track energy value of E_S = 1.25 J/mm
		LR	Not applied			
V11	90	1st	800	640	1.25	
		LR	Not applied			
V12	60	1st	1,000	1,000	1.0	Influence of LR-application on the melt pool depth and comparison with state of the art
		LR	1,000	1,000	1.0	
V13	60	1st	800	640	1.25	
		LR	800	640	1.25	

3 Results and discussion

Figure 9 shows cross sectional images of reference samples manufactured with the V1 parameter set. The shown images are representative for the four reference samples. All reference samples showed two types of pores. The first type of pores exhibited a maximum size below 50 µm and thus was smaller than the melt pool itself, *Fig. 9 a)* and *b)*. The porosity of the V1 samples due to the first type of pores (size below 50 µm) was in the range of 0.18 %. This porosity range correlates with the expectation for the V1 parameter set and the experience of the previous studies with this parameter set. Therefore, these pores are considered to be conventional PBF-LB pores and represent the porosity value when using powder as delivered without agglomerates. The second type of pores exhibited an average size of several hundred microns and thus these pores were bigger than the melt pool itself, *Fig. 9 c)*. These pores are considered to be the result of powder agglomerates. The overall porosity value of the reference samples considering both types of porosity types was in the range between 0.66 % and 1.87 %.

For the evaluation of the melt pool depth, the original interface was first determined. For this purpose, the edges of the build plate to the left and right of the AM-part were

connected by a line as shown in *Figure* 9 *a)*. This line was considered to represent the original interface. The average melt pool depth was calculated by adding the respective layer height to the average root penetration depth, *Fig. 9 b)*. To consider the distribution of the melt pool depth, the root penetration depth was measured at ten evenly distributed points along the interface.

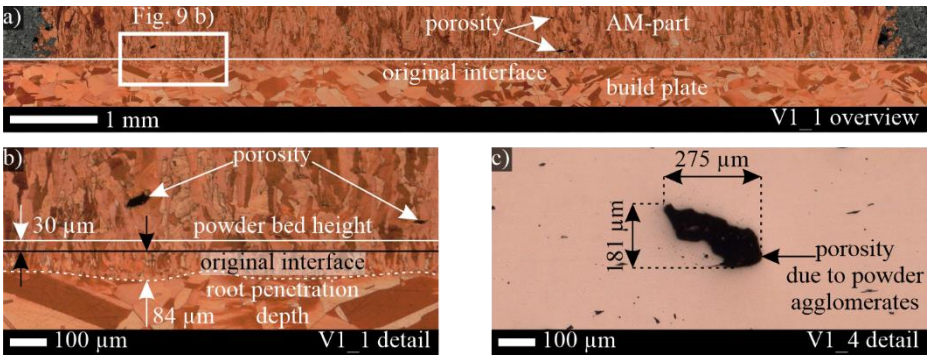

Figure 9: Cross sectional images of reference samples: a) overview image of the interface showing first type of porosity, b) detailed image of the interface showing the methodology for evaluation of the melt pool depth and c) detailed image showing second type of porosity

The described methodology was applied to measure the melt pool depth of all samples. *Figure 10* depicts the influence of the layer height on the melt pool depth, and the melt pool depth of the reference sample. In detail the measured melt pool depth was 107 ± 3.1 µm for V1 ($h_{L,1}$ = 30 µm), 119.5 ± 6.8 µm for V2 ($h_{L,2}$ = 60 µm), and 153 ± 5.4 µm for V3 ($h_{L,3}$ = 90 µm). Thus, an increase of the layer height resulted in an increase of the melt pool depth. Due to the pouring density which is lower than the density of bulk material the powder bed has a lower mass than the build plate. Therefore, less energy is necessary for melting of the powder layer than of the build plate mass with the corresponding height. Thus, an increase of the layer height results in the increase of the total melt pool depth. *Table 3* shows exemplary this effect on the base of a volume with a base area of A = 100 µm², an overall height of h_O = 100 µm, and different powder bed layer heights of $h_{L,1}$ = 30 µm and $h_{L,2}$ = 90 µm. Here an exemplary pouring density of 50 % of the powder bed and an exemplary material density of ρ = 1 g/µm³ for both powder and build plate was considered. An exemplary melting energy of 1 J/g was assumed.

Table 3: Exemplary comparison of the required melting energy for two volumes with the same height but different powder bed heights

	Low layer height	High layer height
Considered overall height [µm]	100	100
Powder layer height [µm]	30	90
Pouring density [%]	50	50
Mass of powder bed [g]	1,500	4,500
Height of build plate [µm]	70	10
Mass of bulk material [g]	7,000	1,000
Overall mass [g]	8,500	5,500
Melting energy [J]	8,500	5,500

For the reference sample V1, corresponding to a track energy of $E_{T,V1}$ = 0.8 J/mm and a nominal layer height of 30 µm, a melt pool depth of 107 ± 3.1 µm was measured at the interface between the base plate and the AM-part, *Figure 10*. Therefore, the first layers of

the reference parameter set with the layer height of 30 µm undergo three full melting cycles. Assuming a conservative powder pouring density of 50 % and a fully dense AM part, the subsequent layers, which have a nominal layer height of 30 µm, exhibit a real layer height that converges to 60 µm by the 11th layer. Consequently, V2, with a nominal and real layer height of 60 µm in the interface between the base plate and the AM-part, represents the reference AM-process starting from the 11th layer. Here a melt pool depth of 119 ± 6.8 µm was measured. Since the real layer height of the reference AM-process starting from the 11th layer onwards is approximately 60 µm and the corresponding melt pool depth is 119.5 ± 6.8 µm, each of these layers undergoes only two melting cycles, in contrast to the three melting cycles observed in the initial layers of the same process.

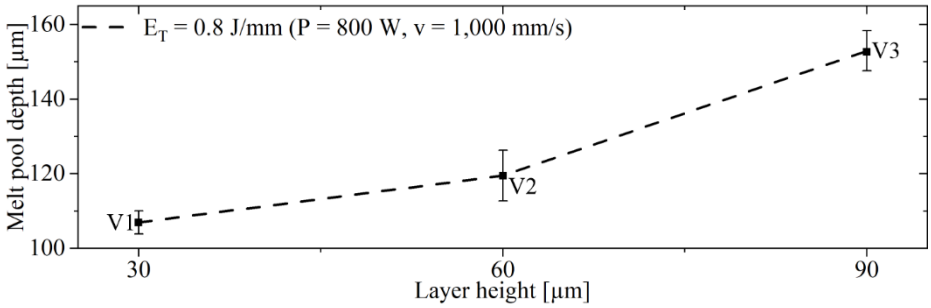

Figure 10: Melt pool depth of the reference parameter set in dependence of the layer height

Regarding the LR approach, these findings indicate that the melt pool depth has to be at least twice the respective nominal layer height in both the initial layers and the subsequent layers to achieve at least the same number of full melting cycles as in the reference process. A melt pool depth of twice the nominal layer height results in four full melting cycles of the initial layers when applying the LR approach, which is one cycle more than the reference process. The first two melting cycles occur during the exposure and LR-exposure of the respective layer, while the additional two cycles arise during the exposure and the LR-exposure of the next layer. For the case of the subsequent layers, a melt pool depth of twice the nominal layer height results, due to the pouring density and thus an increase of the real layer height, in only two full melting cycles, which is the same as for the reference process. Here the melting occurs during the exposure and the LR-exposure of the respective layer.

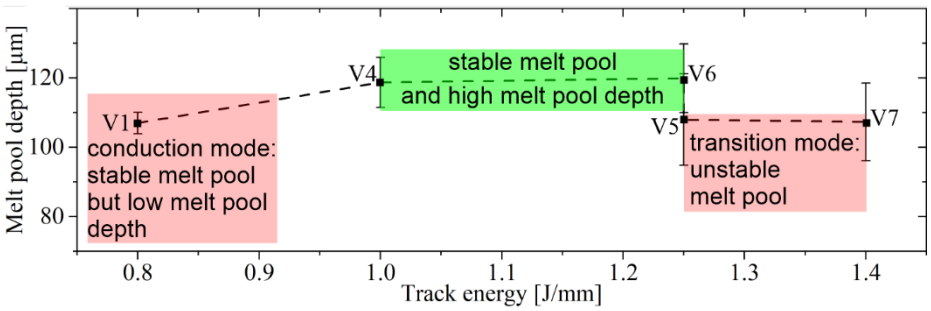

Figure 11: Melt pool depth in dependence of the track energy for a layer height of h_L = 30 µm

Figure 11 shows the measured melt pool depth in the interface between the base plate and the AM-part in dependence of the energy density for a layer height of h_L = 30 µm. For the reference sample V1 and thus a track energy of $E_{T,V1}$ = 0.8 J/mm a melt pool depth of 107 ± 3.1 µm was measured. An increase of the track energy to a value of $E_{T,V4}$ = 1.0 J/mm for the case of V4 resulted in an increase of the melt pool depth to a

value of 118,7 ± 7.2 µm. A further increase of the track energy to a value of $E_{T,V5/V6}$ = 1.25 J/mm resulted in an increase or decrease of the melt pool depth in dependence of the respective combination of laser power and scan velocity. For the case of V6 an average melt pool depth of 119.7 ± 9.9 µm was measured. For the case of V5 an average melt pool depth of 108 µm ± 13.2 µm was measured, which is smaller than that of V1 or V4, despite V5 having the highest track energy. A further increase of the track energy to a value of $E_{S,V7}$ = 1.4 J/mm for the case of V7 resulted even in a lower average melt pool depth of 107.3 ± 11.2 µm.

The decrease of the melt pool depth when increasing the track energy may be attributed to the transition of the melt pool from the conduction to the transition mode. The transition mode is characterized by a partial evaporation of the material from the melt pool, comparable to the keyhole mode at higher energy densities [41]. At the same time a stable keyhole mode is not established yet. Therefore, the transition mode is not stable and the melt pool depth decreases due to a significant energy loss by material evaporation compared to the case of conductive mode. Furthermore, the comparison of V5 and V6 shows that the arise of the transition mode depends not only on the track energy. In fact, the process mode is determined by the entirety of the parameters and their respective combination [41]. Thus, the melt pool depth is limited not only by the resulting roughness values but also the melt pool stability.

Therefore, the parameter sets V5 and V7 resulting in a transition mode melt pool are not suitable for the targeted LR-approach. Since parameter sets V4 and V6 exhibited comparable melt pool depths within the margin of deviation, and significantly greater melt pool depths than parameter set V1, the subsequent investigations were conducted using the laser power and scan velocity of V4 and V6, while varying the layer height.

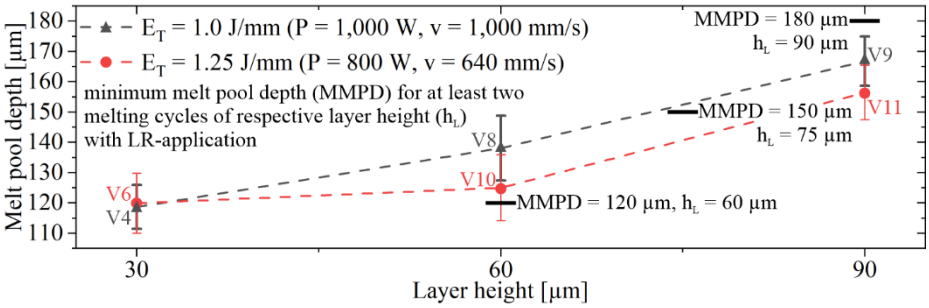

Figure 12: Melt pool depth in dependence of the layer height

Figure 12 shows the influence of the layer height on the melt pool depth. For both cases, a track energy of E_T = 1.0 J/mm (P = 1,000 W, v = 1,000 mm/s) and E_T = 1.25 J/mm (P = 800 W, v = 640 mm/s), an increase of the layer height resulted in an increase of the melt pool depth in the interface between the base plate and the AM-part during the first exposure. For a layer height of h_L = 90 µm the melt pool depth was 166.8 ± 8.1 µm for the case of V9 and 156.4 ± 9 µm for the case of V11. For the case of the initial layers, these melt pool depths result in only two full melting cycles of each layer with the height of 90 µm even with one LR-application. For subsequent layers, the real layer height increases to approximately 180 µm due to the pouring density. Therefore, the measured melt pool depths are considered to be insufficient to completely melt these layers. To ensure at least two complete melting cycles of each layer during the process with an LR application, a minimum melt pool depth of 180 µm is required for a nominal layer height of 90 µm. It may be noted that the melt pool might increase further to the required value for the case of a real layer height of 180 µm instead of the investigated 90 µm. However,

since the measured melt pool depth does not ensure three full melting cycles of the initial layers, as for the reference process, the nominal layer height of 90 µm was not investigated further.

For the case of a layer height of h_L = 60 µm, melt pool depths of 125 ± 10.9 µm and 138.1 ± 10.7 µm for V10 (E_T = 1.25 J/mm) and V8 (E_T = 1.0 J/mm) respectively were measured in the interface. When applying the LR-approach, both parameter sets ensure at least three full melting cycles of the initial layers. For subsequent layers and thus the increase of the real layer height to a value of 120 µm, the minimum required melt pool depth to achieve at least two complete melting cycles with the LR approach is 120 µm. Thus, starting from a real layer height of 60 µm, the track energy of E_T = 1.0 J/mm (V8) ensures a sufficient melt pool depth for two full melting cycles of the process with a nominal layer height of 60 µm and a LR-application. At a track energy of E_T = 1.0 J/mm, the melt pool depth allows at least two full melting cycles of each layer with a nominal height of 60 µm and a LR-application, starting from a real layer height of 90 µm. Therefore, both V8 and V10, each with a nominal layer height of 60 µm, were applied to evaluate the influence of a layerwise LR-application on the melt pool depth and for comparison with the reference sample. The results of the LR-application are depicted in *Figure 13*.

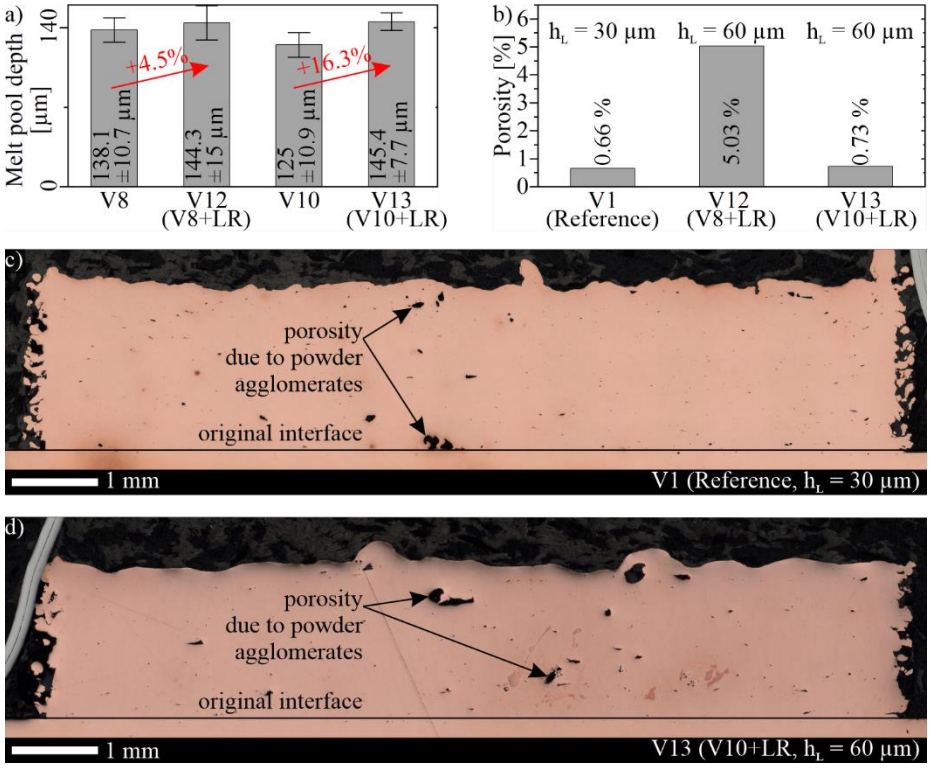

Figure 13: a) influence of LR-application on the melt pool depth, b) porosity values of the reference sample (V1) and effect samples (V12, V13), c) cross sectional image of the reference sample (V1), d) cross sectional image of effect sample (V13)

The application of the LR-approach resulted in an increase in the average melt pool depth of 4.5% and 16.3%, reaching values of 144.3 ± 10.7 µm and 145.4 ± 7.7 µm for V12 and V13, respectively, *Fig. 13 a)*. These results confirm that preheating during the first exposure and the resulting increase in thermal conductivity during subsequent LR-application in the conductive regime have a beneficial effect on melt pool depth and liquid lifetime. *Figure 13 b)* shows the porosity values of the samples V1 (Reference), V12 (V8+LR), and V13 (V10+LR). The reference sample with a layer height of h_L = 30 µm and

a state of the art exposure strategy exhibited a porosity value of 0.66 %. The porosity of V12 with a value of 5.03% is supposed to arise primarily due to the powder quality. For the case of V13 with a layer height of h_L = 60 µm and a layerwise LR-application a porosity value of 0.73 % was measured. Therefore, for the case of V13, a comparable quality regarding the porosity value of the PBF-LB part was achieved by using the LR-exposure strategy, despite a double layer height compared to the reference samples being applied. The porosity values of all three samples resulted mainly from the second type pores, which are assumed to occur due to powder agglomerates as shown in *Figure 13 c)* and *d)*.
For the case of V13 the LR-application resulted in time savings of 28 % due to lower coating time while maintaining comparable part quality as the reference sample which represented the state of the art. To determine the respective process efficiency, the overall exposure time was calculated based on the respective process parameters and a specific part geometry, while the total coating time was calculated based on an experimental determination of the average coating time per layer. The coating time per layer was considered to be the same for both, the reference process and the LR-process. The exposure time was calculated based on an AM-part with a surface area of A = 300 mm^2, a part height of 10 mm, and the respective process parameter sets of V1 (reference) and V13 (LR-approach). The average coating time was determined by recording the time required for 20 coating processes and was t_c = 12 s per coating process. Since the exposure time per unit height for the V13 parameter set is longer than that of the reference parameter set, it should be noted that the stated time savings resulted primarily from the reduced coating time. Thus, the time savings obtained using the V13 parameter set decrease for AM processes with larger base areas, but increase for AM-processes characterized by longer coating times. The time savings of the V13 parameter set are significant up to a part surface area of approximately 1,000 mm^2. Furthermore, based on the results, a reduction in exposure time through a careful optimization of the exposure parameters – for the first exposure and in particular the LR-exposure – along with a further increase of the layer height up to 75 µm, is considered feasible. Therefore, the approach under review is considered to be promising.

4 Summary and outlook

An approach to increase the economic efficiency of PBF-LB processes by applying a LR-exposure strategy when using high layer heights was presented. This approach aims to optimize the respective exposure processes, which are the first and the LR-exposure, regarding either a high melt pool depth enabling the application of high layer heights or to smooth out the roughness peaks to ensure a sufficient surface quality and thus a high powder bed quality of the next layer. The possibility to smooth the surface roughness by LR-application and a high melt pool depth are the basic requirements for this approach. Since surface smoothening by laser polishing represents the state of the art but the melt pool depth in conduction mode is limited by the low thermal conductivity of the powder bed, the possible melt pool depth in the interface between the base material and the AM-part during first exposure of the powder bed and during LR-exposure of AM-layers was evaluated in dependence of the process parameters, including different layer heights and energy densities. It should be noted that the powder used exhibited significant agglomerates, which may introduce deviations compared to the use of virgin powder. Nevertheless, as identical powder quality was used in all experiments, the results are considered as qualitatively comparable. Therefore, the investigated effects of the

parameter sets on the AM-process and on the applicability of the LR-approach are regarded valid. The main findings are the following:

- The possibility to increase the melt pool depth by increasing the track energy in the conduction mode is limited due to the transition mode or the melt pool stability
- Transition mode is characterized by partially material evaporation without a stable keyhole, resulting in a decrease of the melt pool depth
- An increase of the layer height results in an increase of the total melt pool depth due to the pouring density of the powder bed
- In conduction mode the LR-application results in an increase of the melt pool depth due to the preheating effect during the first exposure and a higher thermal conductivity of the onetime melted and consolidated layer during the LR-application

This study aimed to evaluate the applicability of the LR-approach and thus focused on the melt pool depth at the considered exposure processes but not to optimize the smoothing effect of the LR-application yet. Since the applicability is considered to be promising, in the next step, further investigations are necessary to optimize the LR-exposure regarding the smoothing effect which is expected to result in even higher economic efficiency of PBF-LB processes to utilize the full potential of this approach.
Moreover, a track- or double trackwise LR-application with a specific track length instead of a layerwise LR-exposure is supposed to have a positive impact on the PBF-LB process in conduction mode. On the one hand the temperature level is higher when applying the LR-exposure trackwise since the cooling time of the respective track is lower compared to the state of the art or a layerwise LR-application, as described in the chapter 2. This allows an application of low track energy by increasing the scanning time while maintaining an appropriate melt pool depth and thus liquid life time which is decisive for the formation of gas pores. On the other hand, the temperature gradient within the material and thus the marangoni effect which is responsible for the melt pool dynamic is expected to be lower. This is supposed to result in higher surface quality and thus higher smoothing effect of the trackwise LR-application compared to the layerwise LR-exposure.

References

[1] Taghian M, Mosallanejad MH, Lannunziata E, Del Greco G, Iuliano L, Sabori A (2023) Laser powder bed fusion of metallic components: Latest progress in productivity, quality, and cost perspectives. Journal of Materials Research and Technology 27. https://doi.org/10.1016/j.jmrt.2023.11.049

[2] Pettinacci V, Filoscia F, Yadav RP, Cortis D, Cavoto G, Pandolfi F, Orlandi D, Frisenda R, Bracciale MP, Paglia L, Marra F, Rago I (2026) Enhancing copper processability via carbon nanotubes reinforcement in Powder Bed Fusion - Laser Based: Dragon Copper. Materials Today Communications 50. https://doi.org/10.1016/j.mtcomm.2025.114572

[3] Paddock-Lamb R, Khanbolouki P, Cullian MA, Tehrani M (2026) Near-infrared laser powder bed fusion of pure copper: Post-processing and structure–property relationships. Journal of Materials Research and Technology 40. https://doi.org/10.1016/j.jmrt.2025.12.227

[4] Gao S, Qi Y, Bai X, Zhu C, Meng F, Liogas KA, Ramesh A, Yamakawa T, Kumano M, Lee CHT, Zhou K (2025) High-strength and high-conductivity pure copper by powder bed fusion with a medium-power infrared laser. Materials & Design 258. https://doi.org/10.1016/j.matdes.2025.114551

[5] Wong H, Dawson K, Ravi, GA, Howlett L, Jones RO, Sutcliffe C (2019) Multi-Laser Powder Bed Fusion Benchmarking—Initial Trials with Inconel 625. The International Journal of Advanced Manufacturing Technology 105. https://doi.org/10.1007/s00170-019-04417-3

[6] Raut R, Ball MK, Basak A (2025) Impact of track length, track shape, and track location on thermal distortion in laser powder bed fusion of IN625: Single laser vs. three lasers. Journal of Engineering Research 13, 1. https://doi.org/10.1016/j.jer.2023.09.026

[7] Caglar H, Liang A, Groom K, Mumtaz K (2024) Multi-laser powder bed fusion of Ti6Al4V: Diode area melting utilizing low-power 450 nm diode lasers. Journal of Materials Processing Technology 325. https://doi.org/10.1016/j.jmatprotec.2024.118303

[8] Renishaw (2024) New Renishaw technology achieves up to 50% reduction in additive manufacturing build times. https://www.renishaw.com/en/new-renishaw-technology-achieves-up-to-50-reduction-in-additive-manufacturing-build-times--48455. Accessed 29 October 2025

[9] Drechsel K, Lubkowitz V, Albrecht L, Schäfer P, Schneider M, Schulze V, Zanger F (2024) Development of an ultrasonically excited recoating process in laser powder bed fusion to process non-spreadable 316L powder. Powder Technolo-gy, 432. https://doi.org/10.1016/j.powtec.2023.119153

[10] Herzog D, Bartsch K, Bossen B (2020) Productivity optimization of laser powder bed fusion by hot isostatic pressing. Additive Manufacturing 36. https://doi.org/10.1016/j.addma.2020.101494

[11] Feicks SF, Miaskowski CC (2023) Kalibriersystem und Kalibrierverfahren zur Kalibrierung eines Bauplattformsystems in einer additiven Fertigungsvorrich-tung. DE 10 2022 129 042 B3. German Patent and Trade Mark Office. https://depatisnet.dpma.de/DepatisNet/depatisnet?action=pdf&docid=DE102022129042B3. Accessed 29 October 2025

[12] Feicks SF, Miaskowski CC (2024) Bauplattformsystem für die additive Fertigung. DE 10 2022 129 035 A1. German Patent and Trade Mark Office. https://depatisnet.dpma.de/DepatisNet/depatisnet?action=pdf&docid=DE102022129035A1. Accessed 29 October 2025

[13] Schmidt A (2025) Verbesserung der Qualität von additiv gefertigten Bauteilen mittels Entwicklung bedarfsgerechter Strategien zur hybriden Nachprozessierung. DE 10 2023 135 478 A1. German Patent and Trade Mark Office. https://depatisnet.dpma.de/DepatisNet/depatisnet?action=pdf&docid=DE102023135478A1. Accessed 29 October 2025

[14] Cook GO, Sorensen CD (2011) Overview of transient liquid phase and partial transient liquid phase bonding. Journal of Materials Science 46. https://doi.org/10.1007/s10853-011-5561-1

[15] AlHazaa A, Khan TI, Haq I (2010) Transient liquid phase (TLP) bonding of Al7075 to Ti–6Al–4V alloy. Materials Characterization 61, 3. https://doi.org/10.1016/j.matchar.2009.12.014

[16] Atieh AM, Cooke KO, Epstein M (2022) Transient liquid phase (TLP) bonding as reaction–controlled diffusion. Materials Today Communications, 33. https://doi.org/10.1016/j.mtcomm.2022.104293

[17] Hatem Kadrim R, O Al-Roubaiy A, Omidvar H (2024) The effect of post-bond heat treatment on microstructure and mechanical properties of a two-step heating transient liquid-phase bonding IN738LC. Advances in Materials and Processing Technologies. https://doi.org/10.1080/2374068X.2024.2423501

[18] Ghaderi S, Karimzadeh F, Ashrafi A, Hosseini SH (2020) Effect of pressure, temperature and homogenization on the dissolution behavior and mechanical properties of IN718/AISI 304 during transient liquid phase bonding. Journal of Manufacturing Processes, 60. https://doi.org/10.1016/j.jmapro.2020.10.047

[19] Shi X, Ma S, Liu C, Chen C, Wu Q, Chen X, Lu J (2016) Performance of High Layer Thickness in Selective Laser Melting of Ti6Al4V. Materials 9, 12. https://doi.org/10.3390/ma9120975

[20] Wang S, Liu Y, Shi W, Qi B, Yang J, Zhang F, Han D, Ma Y (2017) Research on High Layer Thickness Fabricated of 316L by Selective Laser Melting. Materials 10, 9. https://doi.org/10.3390/ma10091055

[21] Leicht A, Fischer M, Klement U, Nyborg L, Hryha E (2021) Increasing the Productivity of Laser Powder Bed Fusion for Stainless Steel 316L through In-creased Layer Thickness. Journal of Materials Engineering and Performance, 30. https://doi.org/10.1007/s11665-020-05334-3

[22] Brudler A, Medvedev AE, Pandelini C, Piegert S, Illstron T, Qian M, brandt M (2024) Systematic investigation of performance and productivity in laser pow-der bed fusion of Ti6Al4V up to 300 µm layer thickness. Journal of Materials Processing Technology, 330. https://doi.org/10.1016/j.jmatprotec.2024.118450

[23] McConell S, Tanner D, Kourousis KI (2024) Productivity improvement oppor-tunities for metal powder bed fusion technologies: a systematic literature review. Rapid Prototyping Journal 30, 11. https://doi.org/10.1108/RPJ-09-2023-0333

[24] Zhao L, Chu F, Wang Q, Li J, Lin J, Wu X, Hou J (2025) Integration of High Productivity and Mechanical Properties of AISI 420 Stainless Steel Processed by Laser Powder Bed Fusion. Advanced Engineering Materials 27, 12. https://doi.org/10.1002/adem.202500066

[25] Günther I, Zillmann B, Niendorf T (2025) Metal powder bed fusion of pure and coated copper for power electronics applications using a green laser. Journal of Materials Research and Technology 38. https://doi.org/10.1016/j.jmrt.2025.09.007

[26] Mayerhofer M, Brenner S, Dickmann M, Doppler M, Gruber S, Helm R, Lopez E, Maier V, Mitteneder J, Neukirchen C, Nedeljkovic-Groha V, Reinarz B, Schuch M, Stepien L, Dollinger

G (2024) Red and Green Laser Powder Bed Fusion of Pure Copper in Combination with Chemical Post-Processing for RF Cavity Fabrication. Instruments 8, 39. https://doi.org/10.3390/instruments8030039

[27] Ali U, Mahmoodkhani Y, Imani Shahabad S, Esmaeilizadeh R, Liravi F, Shey-daeian E, Huang KY, Marzbanrad E, Vlasea M, Toyserkani E (2018) On the measurement of relative powder-bed compaction density in powder-bed addi-tive manufacturing processes. Materials & Design 155. https://doi.org/10.1016/j.matdes.2018.06.030

[28] Haapa E, Gopaluni A, Piili H, Salminen A, Ottelin J (2023) Validation of powder layering simulation via packing density measurement for laser-based powder bed fusion. IOP Conf. Series: Materials Science and Engineering 1296. https://iopscience.iop.org/article/10.1088/1757-899X/1296/1/012020

[29] Wischeropp TM, Emmelmann C, Brandt M, Pateras A (2019) Measurement of actual powder layer height and packing density in a single layer in selective laser melting. Additive Manufacturing 28. https://doi.org/10.1016/j.addma.2019.04.019

[30] Khairallah SA, Anderson AT, Rubenchik A, King WE (2016) Laser powder-bed fusion additive manufacturing: Physics of complex melt flow and formation mechanisms of pores, spatter, and denudation zones. Acta Materialia 108. https://doi.org/10.1016/j.actamat.2016.02.014

[31] Martin AA, Calta NP, hammos JA, Khairallah SA, Nielson MH, Shuttlesworth RM, Sinclair N, Matthews MJ, Jeffries JR, Willey TM, Lee JRI (2019) Ultrafast dynamics of laser-metal interactions in additive manufacturing alloys captured by in situ X-ray imaging. Materials Today Advances 1. https://doi.org/10.1016/j.mtadv.2019.01.001

[32] Ebrahimi A, Kleijn CR, Richardson IM (2019) The Influence of Surface Defor-mation on Thermocapillary Flow Instabilities in Low-Prandtl Melting Pools with Surfactants. Proceedings of the 5th World Congress on Mechanical, Chemical, and Material Engineering (MCM'19). DOI: 10.11159/htff19.201

[33] Bordatchev EV, Hafiz AMK, Tutnea-Fatan OR (2014) Performance of laser polishing in finishing of metallic surfaces. The International Journal of Advanced Manufacturing Technology 73. https://doi.org/10.1007/s00170-014-5761-3

[34] Marimithu S, Triantaphyllou A, Antar M, Wimpenny D, Morton H, Beard M (2015) Laser polishing of selective laser melted components, International Jour-nal of Machine Tools and Manufacture 95. https://doi.org/10.1016/j.ijmachtools.2015.05.002

[35] Li J, Wu H, Liu H, Zuo D (2023) Surface and property characterization of selec-tive laser-melted Ti-6Al-4V alloy after laser polishing. International Journal of Advanced Manufacturing Technology, 128. https://doi.org/10.1007/s00170-023-11880-6

[36] Du C, Zhao Y, Xu Z, Sun Y (2025) Influence of In Situ Laser Polishing on Pore Defects and Mechanical Properties of IN718 Alloy Fabricated by Selective Laser Melting. Journal of Materials Engineering and Performance, 34. https://doi.org/10.1007/s11665-024-09678-y

[37] Yasa E, Deckers J, Kruth JP (2011) The investigation of the influence of laser re-melting on density, surface quality and microstructure of selective laser melting parts. Rapid Prototyping Journal 5. https://doi.org/10.1108/13552541111156450

[38] Chen J, Song C, Chen Y, Chen H, Han C, Yang Y, Wang Q, Wang J (2025) In-vestigation of laser remelting to overcome the strength-plasticity trade-off of la-ser powder bed fused tantalum. International Journal of Refractory Metals and Hard Materials 133. https://doi.org/10.1016/j.ijrmhm.2025.107351

[39] Chmielewska A, Wysocki BA, Gadalińska E, MacDonald E, Adamczyk-Cieślak B, Dean D, Świeszkowski W (2022) Laser powder bed fusion (LPBF) of NiTi al-loy using elemental powders: the influence of remelting on printability and mi-crostructure. Rapid Prototyping Journal 28, 10. https://doi.org/10.1108/RPJ-08-2021-0216

[40] Schmidt A, Jensch F, Härtel S (2023) Multi-material additive manufacturing-functionally graded materials by means of laser remelting during laser powder bed fusion. Frontiers of Mechanical Engineering 18, 49. https://doi.org/10.1007/s11465-023-0765-z

[41] Assuncao E, Williams S, Yapp D (2012) Interaction time and beam diameter ef-fects on the conduction mode limit. Optics and Lasers in Engineering 50, 6. https://doi.org/10.1016/j.optlaseng.2012.02.001

Contact

Alexander Schmidt (Corresponding author)
Brandenburg University of Technology – Chair of Hybrid Manufacturing
Konrad-Wachsmann-Allee 17, 03046 Cottbus, Germany
E-Mail: alexander.schmidt@b-tu.de
WEB: www.b-tu.de/fg-hybride-fertigung